WOOD RESEARCH doi.org/10.37763/wr.1336-4561/67.6.908918
e-ISSN 2729-8906
67(6): 2022 908-918 pp.

STUDY OF DEWATERING CHARACTERISTICS OF *EUCALYPTUS* WOOD BY SUPERCRITICAL CO_2

HONGHAI LIU, XIAOKAI ZHANG, JINGWEN ZHANG
NANJING FORESTRY UNIVERSITY
CHINA

(RECEIVED JUNE 2022)

ABSTRACT

Wood collapse is a major defect for their applications in solid wood production. Supercritical CO_2 ($ScCO_2$) dewatering can quickly remove water in wood and effectively reduce the capillary tension leading to collapse of wood structure. In this study, *Eucalyptus exserta* F.V. Muell wood was dewatered using $ScCO_2$ at 35, 45, 55°C and 15, 20, 25 MPa, separately. The dewatering characteristics and wood deformation were statistically analyzed and compared after dewatering. The results show that the dewatering rate of $ScCO_2$ is affected by moisture content (MC) of wood, showing the higher the MC, the faster the dewatering. It is also affected significantly by pressure, indicating increased dewatering rate with the pressure. The effect of temperature on dewatering rate is not apparent as the pressure is less than 25 MPa, but it becomes significant at 25 MPa condition, showing an increased dewatering rate with temperature. In this experiment, the greatest dewatering rate was $19.8\%\cdot h^{-1}$ at 55°C and 25 MPa. The transversal shrinkage of all specimens after 5 cycles dewatering was lower than 1.5%, indicating the $ScCO_2$ dewatering could effectively inhibit collapse of eucalyptus wood structure. The transversal shrinkage decreases with the pressure, and is not affected significantly by temperature.

KEYWORDS: Eucalyptus wood, supercritical CO_2, dewatering, characteristics, deformation.

INTRODUCTION

Removing water from wood is important to its utilization because the water affects wood stabilization and service life. Controlled drying operation is a crucial step to improve the physical and mechanical property of wood and maintain wood product quality (Yang et al. 2022, Lyu et al. 2021). A drying method determination is normally based on wood species, timber types, temperatures, cost and end-use requirements. Conventional kiln drying (CKD) of wood is the most widely used method in the world for its efficiency and relatively good quality, but it exhausts steam and volatile compounds derived from thermally treated wood from the kiln, having a negative impact on the environment (Motevali et al. 2014, Fawaz et al. 2020). Additionally, some difficult-to-dry species, such as eucalyptus wood and *poplar* wood, in particular are difficult to dry with CKD methods and usually require a lengthy drying period. The intensive CKD normally results in great negative water tension that develops in boards and leads to a severe collapse during the early stages of drying while still at very high moisture content (MC) **(**Chafe et al. 1992**)**. Thus novel methods to removing water from wood have paid attention to dewatering using mechanical rather than thermal processes.

Supercritical CO_2 ($ScCO_2$), a green and clean solvent, has great potential in the field of wood processing due to its good solubility and strong transfer capacity (Todd et al. 2017, Ferrentino et al. 2018). A solution is proposed for difficult-to-dry wood species to reduce overall drying time and unnecessary deformation. This is a supercritical CO_2 dewatering process which cycles CO_2 between the supercritical state and the gas phase (Franich et al. 2014, Dawson et al. 2015, 2017, Gabitov et al. 2017). Free water in lumens is removed by CO_2 bubbles generated at a decompression process of $ScCO_{2,}$ this leading to a very small gas-liquid interfacial tension (Cao et al. 2021, Yang 2021). Thus, the negative capillary pressure applied to wood cell walls is negligible, and cannot result in collapse of cell wall (Franich et al. 2014, Dawson et al. 2020). Gabitov et al. (2017) had verified that wood shrinkage after dewatering was much smaller than that of CKD and the checking in wood was significantly reduced. Dawson et al. (2020) dried the $ScCO_2$ pre-treated eucalyptus wood using CKD and compared to the wood only suffered CKD, and found that $ScCO_2$ pre-treating can reduce shrinkage by 75%.

China is well of eucalyptus plantations. Certain eucalyptus species with a relatively higher quality have great potential in more wood products (Chen et al. 2019, Zhao et al. 2021, Zhang et al. 2021). Currently, researcher and industries have paid extensive attentions to its high value-added wood products (Zheng et al. 2021, Teixeira et al. 2009, Yang et al. 2018, Yang et al. 2021,). However, most eucalyptus species are prone to collapse and distort during CKD, special treatments (Huang et al. 2020, Kozhin et al. 2012, Franic et al. 2020) are required to improve wood quality and additional functions. Among them, the $ScCO_2$ dewatering has an advantage of clean raw material and technical superiority in fast dewatering. Certain studies on $ScCO_2$ dewatering have been reported, few were related to eucalyptus plantations and to the statistical analysis of dewatering characteristics (Dawson et al. 2017).

In current study, *Eucalyptus exserta* F.V. Muell. wood was dewatered using $ScCO_2$. The dewatering characteristics and wood deformation were statistically analyzed and compared after dewatering. The results will provide technical support for the application of supercritical CO_2 in wood dewatering and collapse-prone species.

MATERIALS AND METHODS

Experiment material

The experimental material was *Eucalyptus exserta* F.V. Muell. The trees were collected in Guangxi province, China, having an average diameter at breast height of 200 mm. They were produced into 1000 mm logs and then delivered to Nanjing Forestry University immediately. The logs were sawn and planed into timbers 30 mm (T) × 30 mm (R) × 1000 mm (L). They were then wrapped tightly with plastic films and stored in a freezer at 4°C. Prior to the $ScCO_2$ dewatering, the timbers were processed into 100 mm long end-matched samples according to the schematic diagram in Fig. 1. The initial MC of each sample was estimated using the two thin slices on both sides of the sample. The average initial MC of the samples were around 62%.

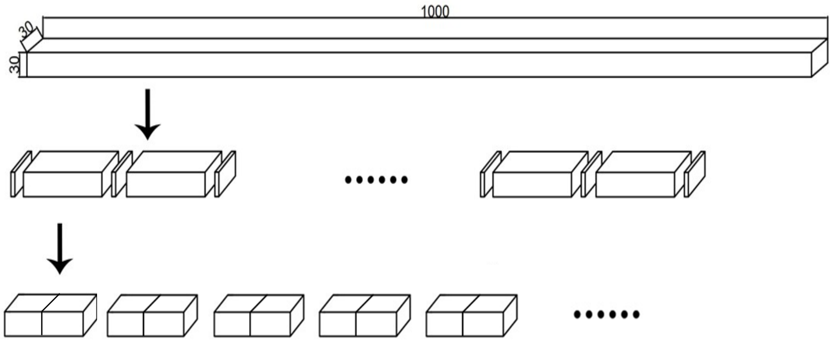

Fig. 1: Schematic diagram of the specimen preparation (units in mm).

Equipment and instruments

The instruments and equipment used in this test are shown in Tab. 1. The $ScCO_2$ plant is the dewatering equipment used in this test. The working schematic diagram is shown in Fig. 2. The $ScCO_2$ dewatering plant is mainly composed of a CO_2 cylinder (1), a circulating pump (2), two dewatering vessels, 5L (3) and 2L (4), and two adsorption vessels (5) and (6).

Tab. 1: Equipment and instruments.

Equipment and Instruments	Model	Manufacturer
$ScCO_2$ plant	DY221-50-06	Jiangsu Nantong Huaan Supercritical Extraction Co., Ltd.
Electronic balance	HC2004(0.001g)	Huachao Hi-Tech Equipment Co., Ltd.
Constant temperature oven	DHG–905386–III	Shanghai Xinmiao Medical Equipment Co., Ltd.
Electronic Vernier caliper	CD-20CPX(0.01mm)	Japan Mitutoyo Co., Ltd.

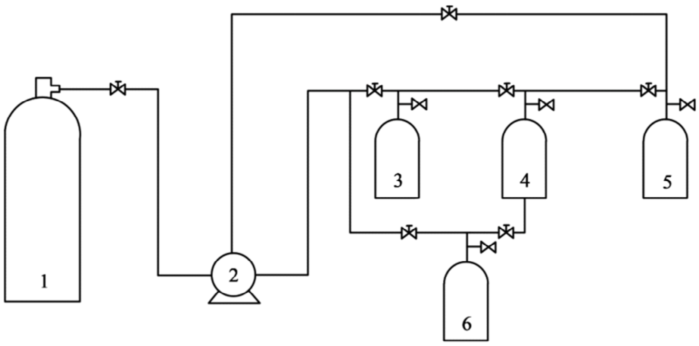

1 CO_2 cylinder, 2 circulating pump, 3 5L dewatering vessel, 4 2L dewatering vessel, 5 and 6 adsorption vessels

Fig. 2: Schematic diagram of the CO_2 dewatering plant.

Experimental method

$ScCO_2$ dewatering of wood

The $ScCO_2$ dewatering parameters in this study are shown in Tab. 2. The steps of one cycle $ScCO_2$ dewatering include: (*1)* Put samples into the 5L dewatering vessel, then close the valve; *(2)* Open the valve of the CO_2 cylinder and pump the CO_2 to the dewatering vessel; *(3)* Heat and compress the CO_2 to the settling values in Tab. 2; *(4)* Maintain the samples in 15 min in the vessel. In this period, the samples were fully contacted with $ScCO_2$; *(5)* Release the $ScCO_2$ in the dewatering vessels to atmosphere until the pressure decreased to 0.1 MPa. The water was removed from wood due to the $ScCO_2$ converts into CO_2 bubbles which expels water out; *(6)* Take samples out from the vessel, then measure the weight and dimensions after CO_2 completely discharged from wood; *(7)* Put samples back into the dewatering vessels for the next dewatering cycle. In this study, totally 5 cycles were repeated for one condition test. After the weight and dimensions measuring in the last dewatering cycle, all samples were dried in an oven at 103°C to obtain the oven-dry mass.

Tab. 2: Process parameters of $ScCO_2$ dewatering.

Process parameters	Numerical value
Maximum pressure (MPa)	15/20/25
Minimum pressure (MPa)	0.1 (atmospheric pressure)
Pressurization time (min)	30
Depressurization time (min)	10
Temperature (°C)	35/45/55
Pressure hold time (min)	15

Moisture content and dewatering rate

The moisture content (MC) of the samples is determined based on the oven-dry method of GB/T 1931-2009. The $ScCO_2$ dewatering rate is calculated according to Eq. 1:

$$R=(M_{\mathrm{i}}-M_{\mathrm{f}})\ /\mathrm{t} \tag{1}$$

where: R- dewatering rate ($\%\cdot h^{-1}$); M_{i} - MC of samples before dewatering (%); M_{f} - MC of samples after dewatering (%); t- dewatering time (h).

Deformation measurement

As shown in Fig. 1, lines were marked along the tangential and radial directions in the middle of the samples. The tangential and radial dimensions were measured using an electronic Vernier caliper before and after each dewatering cycle. The transversal shrinkage was calculated by Eq. 2 and was used to present the dimensional deformation of the samples:

$$\beta =(A_{\mathrm{i}}-A_{\mathrm{f}})\ /\ A_i \tag{2}$$

where: β- transversal shrinkage (%); A_{i} - area of the sample before dewatering (mm^2); A_{f} - area of the sample after dewatering (mm^2).

Statistical analysis

One-way analysis of variance was performed on the data using IBM SPSS Statistics software. If the P value of the analysis of variance was less than 0.05, it was considered that the results were different due to different experimental conditions, that is, the difference between groups was significant.

RESULTS AND ANALYSIS

$ScCO_2$ dewatering curves

Fig. 3 shows the curves of moisture content versus dewatering cycles in the $ScCO_2$ dewatering process. Tab. 3 summarizes the initial MC, final MC and dewatering rates of wood under different conditions.

Tab. 3: Initial MC, final MC and dewatering rate of wood under different conditions.

Dewatering conditions	Initial MC (%)	Final MC (%)	Dewatering rate ($\%\cdot h^{-1}$)
35°C/15 MPa	61.08	51.59	7.59
45°C/15 MPa	56.26	46.44	7.86
55°C/15 MPa	62.15	52.54	7.69
35°C/20 MPa	64.58	51.71	10.30
45°C/20 MPa	70.62	52.04	14.86
55°C/20 MPa	59.72	47.12	10.08
35°C/25 MPa	65.64	55.73	7.93
45°C/25 MPa	59.89	41.59	14.64
55°C/25 MPa	67.53	42.78	19.80

It can be seen in Fig. 3, the MC of the samples decrease fast in the first two cycles and became slow in the subsequent several cycles. The MC decreased from 9.49% (35°C/15 MPa) to 24.75% (55°C/25 MPa) (Tab. 3), indicating that $ScCO_2$ can remove free water from wood quickly and effectively.

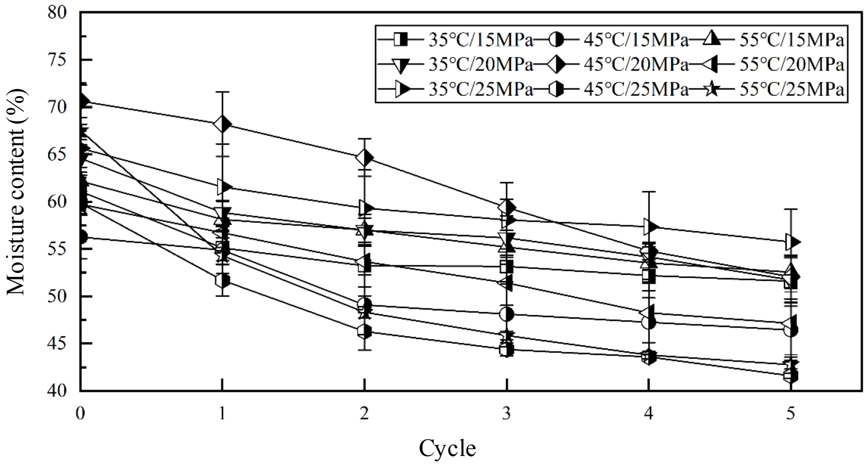

Fig. 3: $ScCO_2$ dewatering curves in five cycles.

Previous study (Behr et al. 2014) also verified the fast dewatering rate of $ScCO_2$ dewatering. They concluded that the MC decrease between 40% and 50% in the first two cycles for wood with initial MC over than 100%. However, the initial MC in this study was around 62%, which was much lower than 100%. This indicates that initial MC of wood influence the dewatering rate, in generally, the higher MC, the greater dewatering rate. The MC decreased became slowly in Fig. 3 in the last three cycles, indicating dewatering rate declines apparently with MC decrease of wood.

Effect of temperature and pressure on $ScCO_2$ dewatering rate

Fig. 4 shows the effect of temperature and pressure on $ScCO_2$ dewatering rate. In the same temperature, the dewatering rate increased with pressure, showing similar variation tendency when the temperatures are between 35 and 55°C.

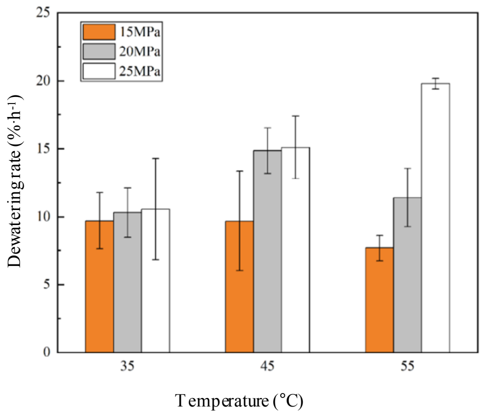

Fig. 4: Effect of temperature and pressure on $ScCO_2$ dewatering rate.

The $ScCO_2$ dewatering process consists of pressurization, pressure hold and depressurization steps. Liquid CO_2 changes into $ScCO_2$ during the pressurization step. The $ScCO_2$ fully contacted with wood samples, penetrates into wood, and dissolves much more free water during the pressure hold step. During the depressurization step, the $ScCO_2$ converts into CO_2 bubbles, resulting in great pressure difference, which expels free water out of wood (Franich et al. 2014). Thus, the higher dewatering rate in higher pressure attributes to the greater pressure difference during the depressurization step. Moreover, the pit membranes were broken up due to the tremendous pressure difference (Newman et al. 2016), resulting in improvement of wood permeability. This accelerates the removal of moisture (Matsunaga et al. 2005, Xiao et al. 2009, Xu et al. 2021, Yang et al. 2021). It also can be seen that in low temperature of 35°C, the effect of pressure on dewatering is not evident, while it becomes significant as temperature excess 45°C, especially for the 55°C conditions. Tab. 4 also indicates that dewatering rate is significantly affected by the pressure at 55°C ($P < 0.05$).

Tab. 4: Pressure-dewatering rate one-way analysis of variance (ANOVA).

Factor	Degrees of freedom	Sum of square	Mean square	F value	P value	Significant
Pressure (35°C)	2	3.076	1.538	0.432	0.662	Not significant ($P > 0.05$)
Pressure (45°C)	2	64.807	32.404	5.487	0.250	Not significant ($P > 0.05$)
Pressure (55°C)	2	322.056	166.028	113.782	0.000	Significant ($P < 0.05$)

At the condition of 15 MPa, the temperature has no significant effect on dewatering rate, however, with the improvement of pressure, a significant effect of temperature on dewatering rate was found, indicating a tendency of increasing of dewatering rate with temperature, especially for the 25 MPa condition. It also can be seen in Tab. 5, the effect of temperature on the dewatering rate is not significant at a low pressure of 15 MPa, but it became significant when pressure was at 20 to 25 MPa. The increased temperature improves solubility of water in $ScCO_2$ (Jiang et al. 2014), leading to more water dissolving in $ScCO_2$, this benefiting for dewatering of water in wood. However, an increase of pressure reduces the solubility of water in $ScCO_2$, thus the temperature and pressure have an interactive effect on the dewatering rate.

Tab. 5: Temperature-dewatering rate two-way analysis of variance (ANOVA).

Factor	Degrees of freedom	Sum of square	Mean square	F value	P value	Significant
Temperature (15 MPa)	2	11.664	5.832	1.258	0.332	Not significant (P > 0.05)
Temperature (20 MPa)	2	55.391	27.695	8.134	0.008	Significant (P < 0.05)
Temperature (25 MPa)	2	198.991	99.495	31.418	0.000	Significant (P < 0.05)

Effects of $ScCO_2$ dewatering on wood deformation

Fig. 5 is the transversal shrinkage after $ScCO_2$ dewatering, indicating the effect of $ScCO_2$ pressure and temperature on the deformation of the *Eucalyptus* samples. After dewatering, all transversal shrinkage ranged from 0.12% to 1.45%, showing a very small shrinkage. This indicates wood has almost no shrinkage in the tangential and radial directions during the dewatering process.

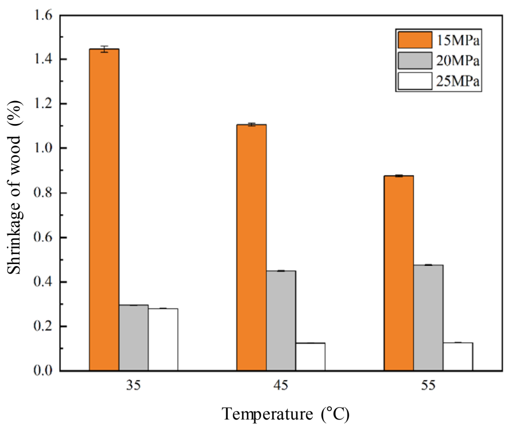

Fig. 5: Effects of temperature and pressure on wood deformation.

Similar results were also found in previous study (Dawson et al. 2017). This shrinkage agrees exactly with the shrinkage rule of normal wood species, i.e., wood dose not shrink as its MC is over fiber saturated point (FSP). However, *Eucalyptus exserta* F.V. Muell. wood is a species that is prone to collapse, and its deformation mainly occurs above FSP during conventional drying process (Yang et al. 2018, 2020). The deformation normally results in severe collapse of wood structure, leading to a lower wood quality. In this study, MC of all samples are all over than FSP after 5 dewatering cycles, however, the total shrinkage were very small compared with other drying approaches. This indicates that $ScCO_2$ dewatering can effectively prevent the collapse of wood structure due to the different mechanism of water removal. The collapse becomes severe due to water migration pathway obstruction or narrowing (Wang et al. 2013). The pressure difference increases with improved dewatering pressure during the depressurization step, which clean and dredge the sediments stored in pits, vessels, and rays. Collapse decreases due to the improvement of water migration pathway in wood.

The deformation of wood at 15 MPa was greater than other two pressure conditions. The transversal shrinkage increased with temperature and shows significant difference ($P < 0.05$) at different temperatures. However, for other two pressures, there were no significant differences ($P < 0.05$) even the temperatures were different. The same results were also observed in Tabs. 6 and 7 based on the statistical analysis. The pressure has significant effect on transversal shrinkage when temperature was at 45 and 55°C, but it has no significant effect on transversal shrinkage for all pressure conditions in this experiment.

Tab. 6: One-way ANOVA of pressure- transversal shrinkage.

Factor	Degrees of freedom	Sum of square	Mean square	F value	P value	Significant
Pressure (35°C)	2	0.527	0.264	1.431	0.323	Not significant ($P > 0.05$)
Pressure (45°C)	2	1.866	0.933	4.580	0.047	Significant ($P < 0.05$)
Pressure (55°C)	2	1.410	0.705	10.979	0.002	Significant ($P < 0.05$)

Tab. 7: One-way ANOVA of temperature-transversal shrinkage.

Factor	Degrees of freedom	Sum of square	Mean square	F value	P value	Significant
Temperature (15 MPa)	2	0.235	0.118	0.421	0.667	Not significant ($P > 0.05$)
Temperature (20 MPa)	2	0.048	0.024	0.873	0.459	Not significant ($P > 0.05$)
Temperature (25 MPa)	2	0.034	0.017	2.256	0.175	Not significant ($P > 0.05$)

CONCLUSIONS

In this study, the $ScCO_2$ dewatering experiments were carried out on *Eucalyptus exserta* F.V. Muell. wood under the conditions of 35, 45, 55°C and 15, 20, 25 MPa, respectively. The results shows that the moisture content (MC) of *Eucalyptus exserta* F.V. Muell. wood decreased between 9.49% and 24.75% within 75 min after 5 dewatering cycles. The dewatering rate of $ScCO_2$ is affected by the MC of wood, showing the higher the MC, the faster the dewatering. The pressure has a significant effect on the dewatering rate when the temperature is between 35 and 55°C, showing an increased dewatering rate with pressure. The rule of temperature on the dewatering was not apparent. Only at 25 MPa, the dewatering rate increased significantly with temperature. In this experiment, when the temperature was 55°C and the pressure was 25 MPa, the dewatering rate of the *Eucalyptus exserta* F.V. Muell. wood had the highest value of $19.8\%\cdot h^{-1}$. The transversal shrinkage of *Eucalyptus exserta* F.V. Muell. wood was less than 1.5%, indicating that $ScCO_2$ dewatering can effectively inhibit the collapse of wood structure. The transversal shrinkage decreased with an increase of pressure, and the temperature had no significant effect on transversal shrinkage. The $ScCO_2$ dewatering is a technique with a rapid water removal and an effective reduction of wood collapse.

ACKNOWLEDGEMENTS

This study was financially supported by the National Natural Science Foundation of China (Grant No. 31870545 and 31570558) and Nanjing Forestry University Undergraduate Innovation Training Project (2021NFUSPITP0700).

REFERENCES

1. Yang, L., Zheng, J.T., Huang, N., 2022: The characteristics of moisture and shrinkage of *Eucalyptus urophylla* × *E. grandis* wood during conventional drying. Materials 15(9): 3386.
2. Lyu, H., Ding, T., Cheng, Y.F., Jiang, N., 2021: Life cycle assessment of kiln-dried oak lumber. Journal of Forestry Engineering 6(5):39-45.
3. Motevali, A., Minaei, S., Banakar, A., Ghobadian, B., Khoshtaghaza, M.H., 2014: Comparison of energy parameters in various dryers. Energy Conversion and Management 87: 711-725.
4. Fawaz, M., Lautenberger, C., Bond, T.C., 2020: Prediction of organic aerosol precursor emission from the pyrolysis of thermally thick wood. Fuel 269: 117333
5. Chafe, S., Barnacle, J., Hunter, A., Ilic, J., Northway, R., Rozsa, A., 1992: Collapse: An introduction. CSIRO, Division of Forest Products, Melbourne, 9 pp.
6. Todd, R., Baroutian, S., 2017: A techno-economic comparison of subcritical water, supercritical CO_2 and organic solvent extraction of bioactives from grape marc. Journal of Cleaner Production 158: 349-358.
7. Ferrentino, G., Morozova, K., Mosibo, O.K., Ramezani, M., Scampicchio, M., 2018: Biorecovery of antioxidants from apple pomace by supercritical fluid extraction. Journal of Cleaner Production 186: 253-261.
8. Franich, R.A., Gallagher, S., Kroese, H., 2014: Dewatering green sapwood using carbon dioxide cycled between supercritical fluid and gas phase. Journal of Supercritical Fluids 89: 113-118.
9. Dawson, B.S.W., Pearson, H., Kroese, H.W., Sargent, R., 2015: Effect of specimen dimension and pre-heating temperature on Supercritical CO_2 dewatering of radiata pine sapwood. Holzforschung 69: 421-430.
10. Gabitov, R.F., Khairutdinov, V.F., Gumerov, F.M., Gabitov, F.R., Zaripov, Z.I., Gaifullina, R., Farakhov, M.I., 2017: Drying and impregnation of wood with propiconazole using supercritical carbon dioxide. Russian Journal of Physical Chemistry B 11: 1223-1230.

11. Dawson, B.S.W., Pearson, H., 2017: Effect of supercritical CO_2 dewatering followed by oven-drying of softwood and hardwood timbers. Wood Science and Technology 51: 771-784.
12. Cao, M.D., Zhang, X.X., Ren, W.T., Zhu, J.W., Wang, H.K., Xu, H.C., Yu, Y., 2021: Effect of drying methods on the cell wall pore structure of *Phyllostachys edulis*. Journal of Forestry Engineering 6(6): 58-65.
13. Yang, L., 2021: Effect of temperature and pressure of supercritical CO_2 on dewatering, shrinkage and stresses of eucalyptus wood. Applied Sciences 11(18): 8730.
14. Dawson, B.S.W., Pearson, H., Kimberley, M.O., Davy, B., Dickson, A.R., 2020: Effect of supercritical CO_2 treatment and kiln drying on collapse in *Eucalyptus nitens* wood. European Journal of Wood and Wood Products 78: 209-217.
15. Chen, Y., Zhu, J., 2019: Study on bending characteristics of fast growing eucalyptus bookcase shelves by using burgers model. Wood Research 64(1): 137–144.
16. Zhao, X.Y., Huang, Y.J., Fu, H.Y., Wang, Y.L., Wang, Z., Sayed, U., 2021: Deflection test and modal analysis of lightweight timber floors. Journal of Bioresources and Bioproducts 6(3): 266–278.
17. Zhang, L., Chen, Z.H., Dong, H.R., Fu, S., Ma, L, Yang, X.J., 2021: Wood plastic composites based wood walls structure and thermal insulation performance. Journal of Bioresources and Bioproducts 6(1): 65–74.
18. Yang, L., Liu, H.H., 2018: A review of eucalyptus wood collapse and its control during drying. BioResources 13: 2171–2181.
19. Yang, L., Jin, H.H., 2021: Effect of heat treatment on the physic-mechanical characteristics of *Eucalyptus urophylla* S.T. Blake. Materials 14(21): 6643.
20. Zheng, X., Deng, Y., LI, Y.Z., Zhu, X.M., 2021: Design and experiment of pruning machine for eucalyptus trees. Journal of Forestry Engineering 6(2): 148–156.
21. Teixeira, T.O.B., Silva, M.L., Jacovine, L.A.G., Valverde, S.R., Silva, J.C., Pires, V.A.V., 2009: The perception of manufacturers of the furniture center of UBA-MG about the use of eucalyptus wood. Revista Arvore 33(5): 969–975.
22. Huang, C., Chui, Y.H., Gong, M., Chana, F., 2020: Mechanical behavior of wood compressed in radial direction: Part II. Influence of temperature and moisture content. Journal of Bioresources and Bioproducts 5(4): 266-275.
23. Kozhin, V.P., 2012: Centrifugal dewatering and drying of high-moisture wood. Journal of Engineering Physics and Thermophysics 85: 1278–1283.
24. Franic, H.R.A., Meder, R., Behr, V.C., 2020: Dewatering green sapwood using carbon dioxide undergoing cyclical phase change between supercritical fluid and gas. Molecules 25(22): 5367.
25. Behr, V.C., Hill, S.J., Meder, R., Sandquist, D., Hindmarsh, J.P., Franich, R.A., Newman, R.H., 2014: Carbon-13 NMR chemical-shift imaging study of dewatering of green sapwood

by cycling carbon dioxide between the supercritical fluid and gas phases. Journal of Supercritical Fluids 95: 535-540.
26. Newman, R.H., Franich, R.A., Meder, R., Hill, S.J., Kroese, H., Sandquist, D., Hindmarsh, J.P., Schmid, M.W., Fuchs, J., Behr, V.C., 2016: Proton magnetic resonance imaging used to investigate dewatering of green sapwood by cycling carbon dioxide between supercritical fluid and gas phase. Journal of Supercritical Fluids 111: 36-42.
27. Matsunaga, M., Matsunaga, H., Kataoka, Y., Matsui, H., 2005: Improved water permeability of sugi heartwood by pretreatment with supercritical carbon dioxide. Journal of Wood Science 51: 195-197.
28. Xiao, Z.P., Lu, X.N., Lu, J.S., 2009: Effects of co-solvent in supercritical CO_2 treatment on wood permeability. Journal of Fujian College of Forestry 29(2): 178-182.
29. Jiang, C.Y., Wu, J.F., Sun, Z.J., Pan, Q.M., 2014: Solubility of water in supercritical CO_2. Chemical Engineering 7: 42-47.
30. Wang, M.X., He, Q., Zhao, X.L., 2013: Study on drying and collapse properties of eucalypts plantation. Journal of Inner Mongolia Agricultural University 34(1): 123-127.
31. Xu, W., Chen, P., Yang, Y., Wang, X., Liu, X., 2021: Effects of freezing and steam treatments on the permeability of *Populus Tomentosa*. Materialwissenschaft und Werkstofftechink 52(8): 907-915.
32. Yang, Y.Q., Xu, W., Liu, X., Wang, X.D., 2021: Study on permeability of *Cunninghamia Lanceolata* based on steam treatment and freeze treatment. Wood Research 66(5): 721-731.
33. Yang, L., Han, T.Q., Fu, Y.D., 2020: Effect of heat treatment and wax impregnation on dimensional stability of *Pterocarpus Macrocarpus* wood. Wood Research 65(6): 963-974.

HONGHAI LIU[1,2*]
NANJING FORESTRY UNIVERSITY
[1]COLLEGE OF FURNISHING AND INDUSTRIAL DESIGN
[2]JIANGSU CO-INNOVATION CENTER OF EFFICIENT PROCESSING AND UTILIZATION OF FOREST RESOURCES
NANJING 210037
CHINA
* Corresponding author: liuhonghai2020@njfu.edu.cn

XIAOKAI ZHANG, JINGWEN ZHANG
NANJING FORESTRY UNIVERSITY
[1]COLLEGE OF FURNISHING AND INDUSTRIAL DESIGN
NANJING 210037
CHINA